Annals of Nuclear Energy 99 (2017) 54–57

Contents lists available at ScienceDirect

Annals of Nuclear Energy

journal homepage: www.elsevier.com/locate/anucene

Technical note

On the equivalence of neutron source and flux spectra

Gašper Žerovnik *, Jure Beričič, Luka Snoj

Jožef Stefan Institute, Jamova cesta 39, SI-1000 Ljubljana, Slovenia

ARTICLE INFO

Article history:
Received 8 April 2016
Received in revised form 5 September 2016
Accepted 13 September 2016

Keywords:
Neutron density
Neutron flux
Neutron source
Neutron transport
Monte Carlo codes
MCNP
^{252}Cf fission spectrum

ABSTRACT

The equivalence between the neutron source and flux spectra is often implicitly used in practice although many times the users are not even aware of this. This work identifies two conditions under which the equivalence holds. Namely, if the neutron interaction between the source region and the volume where flux is observed is negligible, and the neutron mean track length in the observed volume does not depend on their energy, source and flux spectra are equivalent. Consequently, a flux determined on a closed surface from a full system calculation can be replaced by an equivalent source for a simplified model including only the region contained by the surface.

© 2016 Elsevier Ltd. All rights reserved.

1. Introduction

The equivalence between the neutron source and flux spectra is often implicitly used in practice although many times the users are not aware of the conditions under which this equivalence holds. One example of application is a pre-calculated neutron flux spectrum for definition of a source spectrum in simplified-geometry model for reaction rate calculations (Trkov et al., 2009; Žerovnik et al., 2015; ICSBEP, 2015).

For an arbitrary time-independent neutron transport problem in vacuum, the ratio between the number of source neutrons and any surface or volume averaged neutron flux is independent of neutron energy as long as the spatial and angular distribution of the source neutrons remains unchanged. This is obvious for this particular case (i.e. vacuum) since only geometric parameters define the flux/source ratio. When adding material which interacts with neutrons, energy dependence is introduced in the ratio through energy-dependent probabilities for neutron-nucleus interactions (i.e. energy-dependent neutron induced cross sections).

Furthermore, the time-independent neutron transport in a medium is affected by probabilities for interaction of the neutrons with the surrounding material (reaction cross section) and the system geometry, and not directly on neutron energy (or speed), except for energy-dependent reaction cross sections. Since the volume-averaged neutron flux is proportional to the track length in the volume (so-called track length estimators used in Monte Carlo codes such as MCNP (Goorley et al., 2012)), the neutron flux in an arbitrary energy bin also depends only on the number of neutrons passing the volume, the incoming position and angle, and macroscopic cross section in the volume in case the mean chord length of the volume is not negligible compared to the mean neutron free path in the material. It again does not depend directly on neutron energy/speed but indirectly due to energy-dependent reaction cross sections.

As rigorously shown below, the neutron source spectrum is thus equivalent to the neutron flux spectrum and not to the neutron density spectrum. Neutron density in any point/volume in the system for a monoenergetic source and vacuum or energy independent cross section is inversely proportional to the neutron speed.

Important implication of this finding is that one may directly use the results of a calculated neutron flux for definition of a source in the same geometry to propagate neutrons and save computational time. This work looks at the underlying principles of the flux-source equivalence and tries to determine the conditions that need to be satisfied for this equivalence to hold.

2. Definitions

Angular neutron density (Duderstadt and Hamilton, 1976):

$$n(\vec{r}, \vec{\Omega}, E, t), \tag{1}$$

* Corresponding author at: Institute for Reference Materials and Measurements, EC-JRC-IRMM, Retieseweg 111, B-2440 Geel, Belgium.

E-mail addresses: gasper.zerovnik@ijs.si (G. Žerovnik), jure.bericic@ijs.si (J. Beričič), luka.snoj@ijs.si (L. Snoj).

http://dx.doi.org/10.1016/j.anucene.2016.09.026
0306-4549/© 2016 Elsevier Ltd. All rights reserved.

where $\vec{r}$ is the position of the observed neutron in space, $\vec{\Omega}$ its direction, E its energy and t the time.

Angular neutron flux (Duderstadt and Hamilton, 1976):

$$\Phi(\vec{r}, \vec{\Omega}, E, t) \equiv v(E) n(\vec{r}, \vec{\Omega}, E, t), \tag{2}$$

where $v(E)$ is the neutron speed.

Neutron source spectrum can be expressed as:

$$N(E) = S_0 \nu_s(E), \tag{3}$$

where the S_0 is the neutron source emission rate of the source and $\nu_s(E)\mathrm{d}E$ is the fraction of neutrons emitted with energy between E and $E + \mathrm{d}E$ (so that $\int \nu_s(E)\mathrm{d}E = 1$).

3. Source and flux spectrum equivalence

Let us imagine a monoenergetic neutron source with emission rate $N(E_0)$ with speed $v = \sqrt{2E_0/m_\mathrm{N}}$ located in a volume V.

In a medium with negligible scattering the average neutron density is:

$$n = \frac{Npt_\mathrm{p}}{V}, \tag{4}$$

where t_p measures the neutron's average time-of-flight through the selected volume, and p is the fraction of source neutrons entering the volume V. This time is connected to the average track length in the selected volume l_tr and speed v as:

$$t_\mathrm{p} = \frac{l_\mathrm{tr}}{v}. \tag{5}$$

This means that the neutron density is not proportional only to the source rate N at given energy E_0 but also inversely proportional to the neutron speed (or energy):

$$n = \frac{Npl_\mathrm{tr}}{vV}, \tag{6}$$

On the other hand, the neutron flux by definition equals to:

$$\Phi = N\frac{pl_\mathrm{tr}}{V}. \tag{7}$$

If l_tr and p are energy independent, the flux spectrum is proportional to the source spectrum. This is also demonstrated in Fig. 1.

The assumption of energy independent p is valid for a system where the neutron transport from the source to the volume V is not affected by neutron energy. In practice, this means that the source has to be located within the volume V or optically close to it and there is no significant room return. The assumption of energy independent l_tr is valid if the neutron transport in the volume V is not affected by neutron energy. This is always true for any surface or optically thin volume. It follows that for any neutron transport system, this equivalence can be used to simplify/accelerate the neutron transport calculation in an enclosed region of interest. A full scale model of the neutron transport system can be used to calculate neutron flux on a surface (or thin volume) enclosing the region of interest. The incoming (entering the region of interest) neutron flux can directly be used for definition of a neutron source on the surface of the simplified model of the system including only the region of interest thereby accelerating the calculation procedure.

3.1. Example: Reaction rates in ^{252}Cf spontaneous fission spectrum

The ^{252}Cf is used as a reference neutron source and its spontaneous fission spectrum is well characterized. It can be approximated with a Maxwellian spectrum (Snoj et al., 2012):

$$N(E) = C\sqrt{E \exp\left(-\frac{E}{a}\right)}, \tag{8}$$

where C is normalization constant and $a = 1.42$ MeV is model parameter. Alternatively, one could use the spectrum calculated by a sophisticated nuclear model, like the Madland–Nix model (Madland and Nix, 1983), or use an evaluated neutron spectrum, e.g. from the IRDF-2002 nuclear data library (IAEA, 2003).

The reaction rate of neutrons with a target can be described as:

$$R(\vec{r}) = \int_E \Sigma(\vec{r}, E)\Phi(\vec{r}, E)\mathrm{d}E, \tag{9}$$

where the Σ is the macroscopic cross section for interaction with neutrons. Usually, the neutron flux spectrum needs to be calculated at the target, before the integral can be evaluated. However, as shown in Section 3, in some cases the neutron source spectrum can be directly used instead of the flux. This makes calculations for reference sources, like the ^{252}Cf, more convenient, since only normalization needs to be determined. In such simple cases, computationally expensive Monte Carlo simulation is not needed.

4. Flux/source equivalence in Monte Carlo transport simulations

In Monte Carlo particle transport codes such as MCNP, the total average flux over a volume V_j is calculated as:

$$\phi_j = \int_{V_j} \frac{\mathrm{d}V}{V_j} \int_E \mathrm{d}E \int_{4\pi} \mathrm{d}\Omega \int_t \mathrm{d}t \Phi(\vec{r}, \vec{\Omega}, E, t). \tag{10}$$

In most applications, the system is in a steady state, thus the integration may be performed over the entire time interval. Under this assumption, the quantity ϕ_j is proportional to the neutron flux in a cell j corresponding to the volume V_j. The ϕ_j corresponds to the physical quantity of fluence, i.e. time integrated flux, by definition.

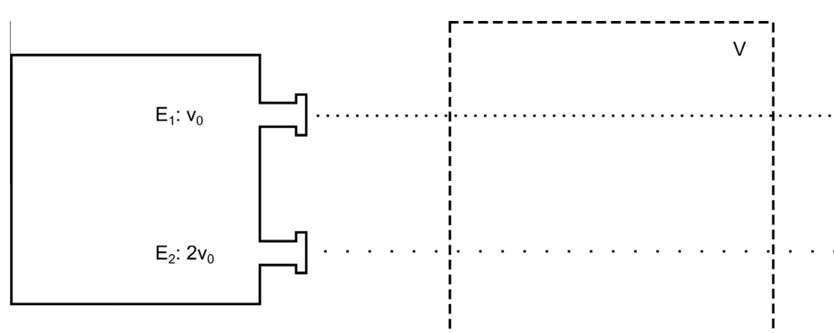

Fig. 1. The neutron source emits neutrons with two energies at the same rate. The density of the slow neutrons in the volume V is higher than that of the fast neutrons. The flux, however, is the same for both.

If the energy spectrum of the flux is needed, the integration can be done over energy bins (intervals) E_k instead over whole energy domain:

$$\phi_{j,k} = \int_{V_j} \frac{dV}{V_j} \int_{E_k} dE \int_{4\pi} d\Omega \int_t dt \Phi(\vec{r}, \vec{\Omega}, E, t). \quad (11)$$

This equation can be rewritten as:

$$\begin{aligned}\phi_{j,k} &= \int_{V_j} \frac{dV}{V_j} \int_{E_k} dE \int_{4\pi} d\Omega \int_t dt\, v(E) n(\vec{r}, \vec{\Omega}, E, t) \\ &= \int_{E_k} dE \int_{4\pi} d\Omega \int_{V_j} \frac{dV'}{V_j} \int_s ds\, n(\vec{r}' + s\vec{\Omega}, \vec{\Omega}, E, t), \end{aligned} \quad (12)$$

where a new variable $s = vt$ was introduced. The time dependence in $n(\vec{r}' + s\Omega, \vec{\Omega}, E, t)$ tracks the paths of neutrons with initial position $\vec{r}'$, direction $\vec{\Omega}$ and energy E. Therefore, the integration over volume dV' should be performed over all possible positions of neutrons at the beginning of the time interval, and depends on energy and direction of travel of the neutrons. Integration over the path s is performed within the chosen cell and the integration limits are functions of energy, direction of travel, and initial position.

From the discrete Monte Carlo treatment of neutrons:

$$n(\vec{r}, \vec{\Omega}, E, t) = \sum_{i=1}^{I} \delta(E - E_i) \delta(\vec{\Omega} - \vec{\Omega}_i) \delta^3(\vec{r} - (\vec{r}_i + v_i t \vec{\Omega}_i)) \quad (13)$$

it follows:

$$\begin{aligned}\phi_{j,k} &= \int_{E_k} dE \int_{4\pi} d\vec{\Omega} \int_{V_j} \frac{dV'}{V_j} \\ &\quad \times \int_s ds \sum_{i=1}^{I} \delta(E - E_i) \delta(\vec{\Omega} - \vec{\Omega}_i) \delta^3(\vec{r}' + s\vec{\Omega} - (\vec{r}_i' + v_i t \vec{\Omega}_i)) \\ &= \sum_{i=1}^{I} \int_{E_k} dE \delta(E - E_i) \int_{V_j} \int_s \frac{dV'}{V_j} ds \delta^3(\vec{r}' - \vec{r}_i') \\ &= \frac{1}{V_j} \sum_{i=1}^{I} w_i^k L_i^j, \end{aligned} \quad (14)$$

where L_i^j is the path length of the i-th neutron in cell j, w_i^k is 1 if neutron is in energy bin k and 0 otherwise, and I is the total number of starting neutrons. Applying the integrals over the solid angle Ω and energy E imply $s = v_i t$ in order for the spatial δ to collapse into the form presented in the second line of Eq. (14).

By normalizing the flux to the number of starting neutrons

$$\varphi_{j,k} = \frac{1}{I} \phi_{j,k} = \frac{1}{V_j} \left(\frac{1}{I} \sum_{i=1}^{I} w_i^k L_i^j \right) \quad (15)$$

it can be seen, that the last part of this equation can be treated as an expected value $w_i^k L_i^j$. If the two factors can be treated as independent variables, than we can use the property $E[XY] = E[X]E[Y]$ of the expected value to write:

$$\varphi_{j,k} = \frac{1}{V_j} \left(\frac{1}{I} \sum_{i=1}^{I} w_i^k \right) \left(\frac{1}{I} \sum_{i=1}^{I} L_i^j \right). \quad (16)$$

This holds when the mean chord length of the cell j as seen by the neutrons does not depend on the energy of the neutrons. The second term in this equation is the fraction of the neutrons with energy in the energy group k or $\nu(E_k)$ and the third term is the mean chord length $\bar{l}_{ch}$:

$$\varphi_{j,k} = \frac{\bar{l}_{ch}}{V_j} \nu(E_k). \quad (17)$$

Comparing this with Eq. (3), it can be seen that the neutron flux as calculated by the track length estimator in Monte Carlo neutron transport codes can be proportional to the source spectrum. Or inversely, that the measured neutron flux spectrum in a cell can, in some cases, be used as an effective neutron source spectrum for that cell. For example, in MCNP this means that the results of the neutron flux calculations by using the track length estimator (F4 tally) represented by neutron flux in multigroup energy format, can be directly used as source definition (SDEF card) in subsequent runs, provided that the tally/source energy and angular resolution and statistical uncertainties are within the acceptable limits for the problem in question.

4.1. Example: Using simplified model for parametric study in a limited region of interest

In Monte Carlo calculations, the user is often interested in observables contained only in a small portion of the system. By taking advantage of the flux/source equivalence it is possible to simplify the model without inducing any biases (however, some statistical uncertainty is propagated while usually not accounted for) in order to save computational time. This can be done in two steps. The primary model includes the full system without the region of interest. The region of interest includes the volume of the calculated quantities and the volume where some parameters may be varied. The region of interest may not include or overlap with the primary source. The primary source can either be a proportional (fission) source or fixed (external) source. The secondary model is the full system model, however without the primary source. The secondary source is located on a surface (or combination of surfaces) enclosing the region of interest.

The inverse can also be done: the initial model including the full system, and the simplified model including only the secondary region (between the secondary source and the region of interest). However, it is not as practical when modifying the secondary region since it yields accurate results only in case that the change of feedback from the secondary to primary region is negligible.

One has to be careful, however, not to increase the number of source particles in secondary calculation beyond the number of detected particles on the secondary source surface from the primary calculation. Otherwise the source particles start to correlate, which is (usually) not accounted for in the final results, therefore the statistical uncertainty may become underestimated.

A very practical example, where this approach is helpful, is when trying to calculate reaction rates in a sample placed in an irradiation channel of a reactor, possibly when using additional internal shielding or transmission filters. The full reactor model is very complex and most simulated neutrons do not even reach the irradiation channel. Therefore, pre-calculating flux at the edge of the irradiation channel and using this as surface source for the secondary calculation can immensely increase the efficiency of the parametric study.

For the proof of concept in this paper, a much simpler artificial spherical model has been chosen (Fig. 2). A 14.1 MeV point neutron source (corresponding to a deuterium–tritium neutron source), shielded by 10 cm of iron and 20 cm of water at normal conditions,

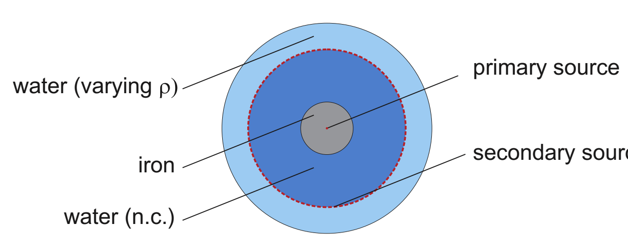

Fig. 2. Components of the spherical full system model.

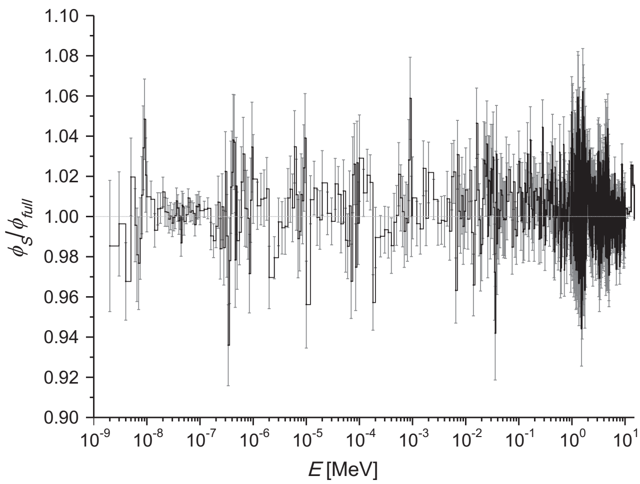

Fig. 3. Ratio of the neutron spectra at radius of 40 cm of the 2-stage model with secondary source at radius of 30 cm to the full system model. 10^7 neutron histories were simulated.

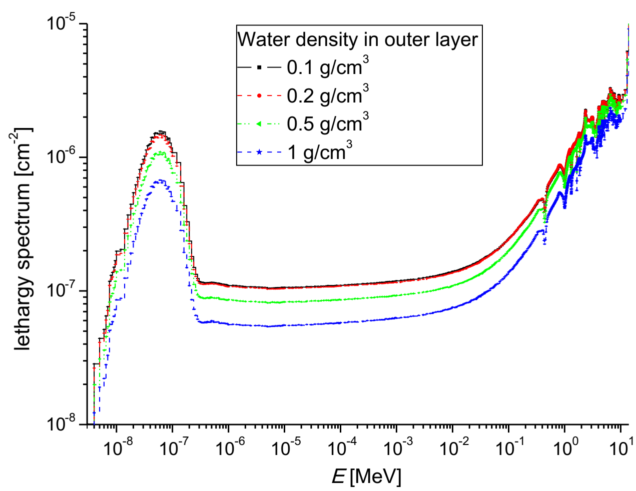

Fig. 4. Neutron lethargy spectra at radius of 40 cm for different densities of water in the outer sphere layer (30–40 cm). The spectra are normalized per one primary source neutron.

was taken as a basis. This was then enveloped into a third sphere of water with varying density and a fixed radius of 40 cm. The surface of the 30 cm sphere has been taken for the secondary source, while the neutron spectrum at 40 cm has been observed as a function of the water density in the outer sphere. Cross sections were adopted from the ENDF/B-VII.1 library (Chadwick et al., 2011).

First, the simplified model has been tested and compared against the full system model. Fig. 3 shows that the variations of the spectrum are mostly within the expected statistical fluctuations. In this particular case, the figure of merit was increased by a factor of 80 in spite of implementing simple variance reduction techniques into the full system model.

After the simplified model was verified, it can freely be used for a parametric study. The neutron spectra corresponding to different water densities in the outer sphere are shown in Fig. 4. In all calculations, the peak from 14.1 MeV fusion neutrons is still present. Expectedly, the full spectrum is lower for higher water densities due to increased absorption, corresponding to a lower fluence per primary source particle.

5. Summary and conclusions

In this work it was shown that under certain conditions, the neutron source and flux spectra are proportional. Two important assumptions were identified: no neutron scattering in the system and neutrons mean track length in the selected volume not depending on their energy.

This equivalence can and already is used in different scenarios, for example using the neutron source spectrum in study of reaction rates or self-shielding of the target, where flux spectrum should be used otherwise. Or inversely, volume- or surface-averaged flux calculated by a Monte Carlo simulation can be used as an effective source spectrum for accelerating localized calculations.

Acknowledgement

This work was supported by the Slovenian Research Agency (ARRS).

References

Chadwick, M.B., Herman, M., Obložinský, P., Dunn, M., Danon, Y., Kahler, A., Smith, D., Pritychenko, B., Arbanas, G., Arcilla, R., Brewer, R., Brown, D., Capote, R., Carlson, A., Cho, Y., Derrien, H., Guber, K., Hale, G., Hoblit, S., Holloway, S., Johnson, T., Kawano, T., Kiedrowski, B., Kim, H., Kunieda, S., Larson, N., Leal, L., Lestone, J., Little, R., McCutchan, E., MacFarlane, R., MacInnes, M., Mattoon, C., McKnight, R., Mughabghab, S., Nobre, G., Palmiotti, G., Palumbo, A., Pigni, M., Pronyaev, V., Sayer, R., Sonzogni, A., Summers, N., Talou, P., Thompson, I., Trkov, A., Vogt, R., van der Marck, S., Wallner, A., White, M., Wiarda, D., Young, P., 2011. ENDF/B-VII.1 nuclear data for science and technology: cross sections, covariances, fission product yields and decay data. Nucl. Data Sheets 112 (12), 2887–2996.

Duderstadt, J.J., Hamilton, L.J., 1976. Nuclear Reactor Analysis. John Wiley & Sons, Inc.

Goorley, J.T. et al., 2012. Initial MCNP6 release overview. Nucl. Technol. 180 (3), 298–315.

IAEA, 2003. International reactor dosimetry file 2002 (IRDF-2002). Technical report series No. 452, International Atomic Energy Agency, Vienna, Austria.

ICSBEP, 2015. ALARM-TRAN-AIR-SHIELD-001, Neutron activation foil and thermoluminescent dosimeter responses to a bare pulse of the CEA Valduc Silene critical assembly. In: International Handbook of Evaluated Critical Safety Benchmark Experiments, Organization for Economic Cooperation and Development – Nuclear Energy Agency.

Madland, D., Nix, J., 1983. Prompt fission neutron spectra and average prompt neutron multiplicities, Report LA-UR-83-3074, Los Alamos National Laboratory, USA.

Snoj, L., Trkov, A., Lengar, I., Popovichev, S., Conroy, S., Syme, B., 2012. Calculations to support {JET} neutron yield calibration: Neutron scattering in source holder. Fusion Eng. Des. 87 (11), 1846–1852.

Trkov, A., Žerovnik, G., Snoj, L., Ravnik, M., 2009. On the self-shielding factors in neutron activation analysis. Nucl. Instrum. Methods Phys. Res. A 610, 553–565.

Žerovnik, G., Kodeli, I.A., Trkov, A., Jazbec, A., 2015. Re-evaluation of the EURACOS integral shielding experiment series. Ann. Nucl. Energy 77, 318–325.